LAWRENCE
LIVERMORE
NATIONAL
LABORATORY

LLNL-PROC-414734

HADS in the Large Magellanic Cloud: Initial findings from the SuperMACHO project

A. Garg

July 15, 2009

Stellar Pulsation: Challenges for Theory and Observation
Santa Fe, NM, United States
May 31, 2009 through June 5, 2009

Disclaimer

HADS in the Large Magellanic Cloud: Initial findings from the SuperMACHO project

Arti Garg and The SuperMACHO Collaboration

Lawrence Livermore National Laboratory, Institute of Geophysics and Planetary Physics, 7000 East Avenue, L-413, Livermore, CA 94550, USA

Abstract.
The SuperMACHO Project is a five-year survey toward the Large Magellanic Cloud (LMC) aimed at understanding the nature of the populations of lenses responsible for the excess microlensing rates observed by the MACHO project [1]. Survey observations were completed in 2006. A rich side-product of this survey is a catalog of variable sources down to a depth of VR 23, including many classes of pulsating variables such as δ-Scuti and RR Lyrae. Through their position in the Period-Luminosity diagram and their light curve characteristics we have identified 2323 high amplitude δ-Scuti (HADS) having high quality light curves. sing Fourier decomposition of the HADS light curves, we find that the period-luminosity (PL) relation defined by the firt-overtone (FO) pulsators does not show a clear separation from the PL-relation defined by the fundamental (F) pulsators. This differs from other instability strip pulsators such as type c RR Lyrae. We also present evidence for a larger amplitude, subluminous population of HADS similar to that observed in Fornax [2].

Keywords: Time series analysis

INTRODUCTION

δ-Scuti variables populate the region of the Hertzprung-Russell diagram where the instability strip meets the main sequence. The high-amplitude variables are generally believed to be pulsating primarily in radial modes, whereas δ-Scuti with smaller amplitudes are believed to have many non-radial modes of pulsation. Until recently, observations of large sets of HADS have been limited due to these stars' intrinsic faintness and short periods. Here we present 2323 candidate HADS in the LMC.

THE SUPERMACHO SURVEY: OBSERVATIONS AND IMAGE REDUCTION

The SuperMACHO project is a five-year optical survey of the Large Magellanic Cloud (LMC) aimed at detecting microlensing of LMC stars [3]. The survey was conducted over 150 half-nights on the CTIO Blanco 4m telescope using a custom *VR* broadband filter with the MOSAIC II wide-field imager. The SuperMACHO survey was completed in January 2006. The 68 SuperMACHO fields cover $\sim$23 deg.^{2} of sky. All survey observations were taken using a single, custom, wide-band, optical filter covering the wavelength range from 5000–7500 Å [see 4, for transmission curve]. Garg et al. [4], Miknaitis et al. [5], Garg [6], and Rest and Garg [7] provide a description of the survey observations and data reduction. We employ a difference imaging technique [see 8, 9] to identify faint variables and obtain cleaner light curves. Garg et al. [4] and Garg et al. (2009, submitted) provide a description of the photometry and variable source identification technique.

In addition to the *VR* survey images, we also obtained a set of high quality *B*- and *I*-band images. We create *B* and *I* catalogs for these images and generate $B-I$ color-magnitude diagrams (CMD) for each field. Though the MOSAIC II camera does not allow for simultaneous imaging in multiple bands, these observations were typically made within 5 minutes of each other. The colors for even relatively short period variables (1-2 hours) should be sufficiently accurate to determine the rough position of sources in the CMD.

DATA AND RESULTS

Candidate Selection

We select candidates based on their position in the period-luminosity (PL) diagram, their position in the $B-I$ CMD, and their amplitude. We perform light curve phasing using both the SuperSmoother algorithm [10] and the CLEANest code [11]. We then apply initial

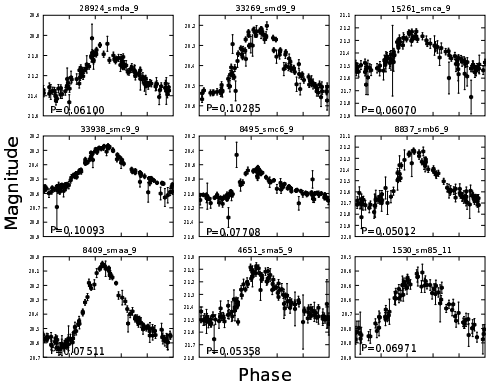

FIGURE 1. Light curves for a selection of δ-Scuti candidates.

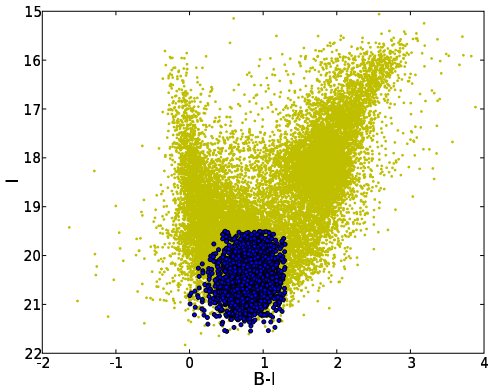

FIGURE 2. $B-I$ color-magnitude diagram. Yellow dots show all star-type sources in the B and I catalog for a single amplifier in field sm97. The CMD is similar for all SuperMACHO fields. The filled blue circles show the final set of HADS candidates.

selection criteria requiring candidates to lie in the region of the PL-diagram associated with δ-Scuti in the LMC ($19.7 < VR < 22.2$ and $0.045 < P < 0.145$ where P is the period in days and VR is the mean VR-band magnitude). We select only sources that appear in the B and I catalogs and lie along the main sequence ($I > 19.5$ mag and 0.0 mag $< B-I < 1.3$ mag). We also require that the minimum difference between the faintest and brightest points on the light curve be greater than 0.2 mag.

After this pre-selection, we use the SigSpec [12] code to determine the frequency spectrum of the light curve. In many cases, the primary frequency of variation found by SigSpec differs from that found during the initial phasing. We use this new frequency to determine the period and select only candidates with 0.045 days $< P < 0.115$ days. We also perform a fourth order Fourier decomposition of the light curves (see below). We use the coeffecient of the zeroth order term, a_0, as the average stellar magnitude and keep candidates with $19.8 < a_0 < 22.2$. Finally, we use the model light curve described by the Fourier fit to determine the overall amplitude, Δ, which we define as the difference between the faintest and brightest points in the model light curve. We select only objects having $\Delta > 0.2$mag.

These selection criteria yield a final set of 2323 HADS candidates. Figure 1 shows a selection of candidate light curves. Figure 2 shows a representative CMD for our LMC fields and the colors of the final HADS candidates.

Fourier Decomposition

Using the period determined by SigSpec, we perform a fourth order Fourier decomposition of the light curve to obtain the coefficients in the series:

$$VR(t) = a_o + \sum_{n=1}^{4} a_n \cos\left(\frac{2\pi nt}{P}\right) + b_n \sin\left(\frac{2\pi nt}{P}\right) \quad (1)$$

where $VR(t)$ is the observed VR magnitude at time t, n counts each order in the decomposition, a_n and b_n are the coefficients of each order determined by the fit, and P is the period. We find that a fourth order expansion is sufficient to capture the structure of the light curves.

Using the Fourier coefficients we calculate several additional parameters describing the light curves. A_n is the amplitude of pulsation for each order such that $A_n^2 = a_n^2 + b_n^2$. r_{ij} is the ratio of amplitudes such that $r_{ij} = A_i/A_j$. ϕ_n is the phase shift for each order such that $\phi_n = atan(b_n/a_n)$. ϕ_{ij} is given by $\phi_{ij} = \phi_i - i\phi_j$.

DISCUSSION

Period-Luminosity diagram

Figure 3 shows the PL diagram of the final HADS candidates. We note that the PL-relation shows a high degree of scatter. This may indicate subgroups within the sample such as the subluminous group observed by [2, hereafter P08]. Because of the possibility of subgroups,

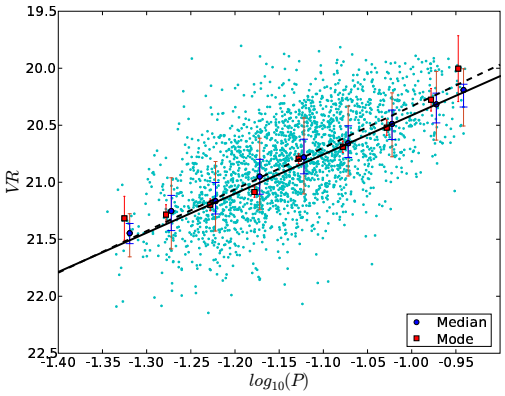

FIGURE 3. PL-diagram of all candidates with fitted PL-relation. The cyan dots show all δ-Scuti candidates. The blue circles give the median magnitudes for each period. The blue and orange error bars show the 33^{rd} and 66^{th} percentiles of the population respectively, i.e. 33% ($\pm$17.5%) and 66% ($\pm$33%) of the candidates within each bin lie between the ends of the error bars. We note that the distribution in each bin is not always symmetric about the median. The red squares show the mode for each bin, and their errors show the inverse square root of the number of sources in the bin. To improve visibility, we show the median and mode values slightly offset from the center of the bin position. The solid line is the best fit PL-relation to the modes (see Equation 3). The dashed black line is the best fit PL-relation when fixing the slope to that given by P08 (see Equation 2).

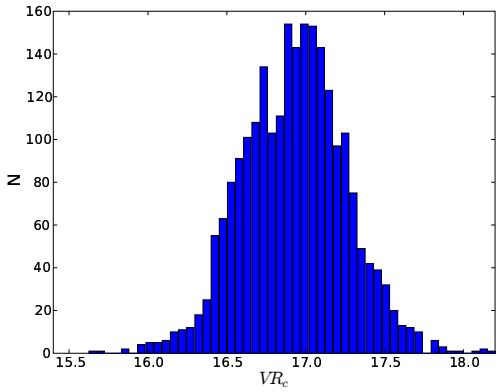

FIGURE 4. Figure showing the histogram of PL-relation-corrected luminosities, VR_c (see Equation 4). We show a histogram for the PL-relation-corrected magnitudes of the candidates using the slope independently determined from this data.

we find the "ridgeline" of the PL-diagram to fit for a PL-relation. This assumes that the main population of δ-Scuti is the most populous. To find the ridgeline we first bin the data by period (0.05 day binsize) and then by VR (20 bins for each period bin). We then take the densest VR bin for each period bin as the mode. We use the inverse square root of the number of candidates in each period bin as the uncertainty. We perform a linear, least-squares fit to the binned data using the slope reported by P08. This yields the PL-relation:

$$VR = -3.65 \log_{10} P + 16.68 \pm 0.11 \text{ mag} \qquad (2)$$

We also independently determine the slope of the PL-relation using the SuperMACHO δ-Scuti. We again perform a fit to the ridgeline, this time leaving the slope as a variable parameter. This fit yields the relation:

$$VR = -3.43 \pm 0.26 \log_{10} P + 16.98 \pm 0.30 \qquad (3)$$

Both fits are shown in Figure 3 Similar to P08, we also determine the PL-corrected luminosity, VR_c, for all candidates using the slope from the best fit. We calculate this value using the relation:

$$VR_c = 3.43 \log_{10} P + VR \qquad (4)$$

Figure 4 shows the histogram of VR_c.

Overtone pulsators

The histogram shown in Figure 4 is heavily skewed toward brighter magnitudes. Typically, such a population that lies above the main PL-relation is thought to be pulsating at the overtone frequency (see P08 and references therein). We consider this hypothesis by examining the relation between VR_c and several parameters describing the candidates' light curves. Figure 5 shows Δ plotted against VR_c. We find that the brightest values of VR_c correspond to the lowest amplitude candidates. Based on observations and models of RR Lyrae, small amplitudes are consistent with the overtone hypothesis [13].

We also examine the shape of the phased light curves using the Fourier components. Based on observations of first-overtone (FO) RR Lyrae, we would expect overtone pulsators to exhibit a more symmetric light curve [14, 15]. By examining the relation between r_{21} and VR_c (Figure 6), we find this to be the case. Because we find that ϕ_{21} is relatively constant for all candidates, r_{21} measures the relative contributions of the second and first fourier components to the overall amplitude. More asymmetric light curves should have higher values of r_{21}, and we find that lower values of VR_c correspond to lower

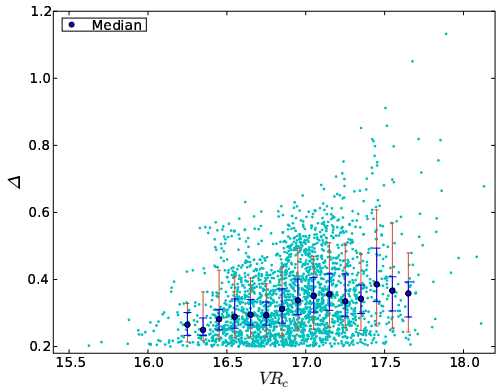

FIGURE 5. Δ against VR_c for all candidates. Δ gives the peak-to-trough amplitude of the phased light curve. We bin the candidates by VR_c. Symbols and error bars are as described in the caption of Figure 3. We do not show bins containing fewer than 20 candidates.

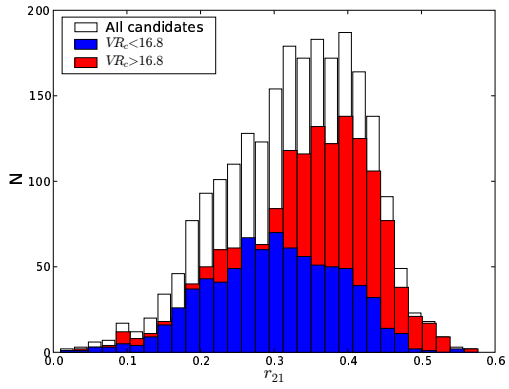

FIGURE 6. Histogram of r_{21} for all candidates. White bars show the histogram of r_{21} for all candidates. Overploted in red are fainter candidates with $VR_c > 16.8$. Overplotted in blue are brighter candidates with $VR_c < 16.8$.

values of r_{21}. This is suggestive that the brighter sources with lower values of r_{21} may be overtone pulsators.

We also note that unlike FO RR Lyrae and FO Cepheids, we see no clear separation between the fundamental (F) and possible FO δ-Scuti. Our results are similar to those of P08 whose PL-diagram also does not show a clear separation. This is not necessarily surprising. δ-Scuti lie in a region of the instability strip that spans a wide range of temperatures and luminosities. Because of this we would expect the PL-diagram to have a broad intrinsic width resulting in regions of FO pulsation that overlap regions of F pulsation.

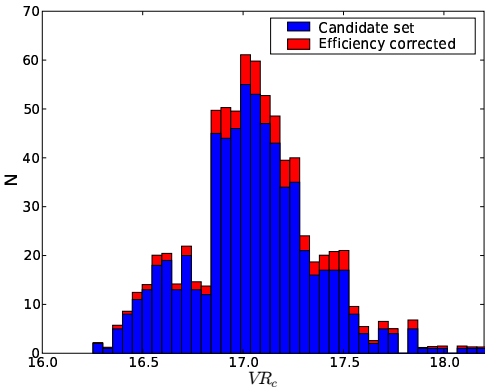

FIGURE 7. Efficiency corrected histogram of VR_c for only sources with $\Delta > 0.4$. The blue bars show the observed histogram, and the red bars give the efficiency-corrected histogram.

Larger amplitude population

The histogram of VR_c shows no strong indication of the subluminous population described in P08. We find, however, that the median Δ increases for fainter sources (Figure 5). To test whether this reflects a selection bias against smaller amplitudes for fainter sources, we use simulations of δ-Scuti light curves similar to those described in Garg [6]. We find that we have a relatively high efficiency for detecting δ-Scuti at all amplitudes and luminosities considered (>65%), and for the faintest sources we are $\sim$ 13% more efficient at detecting larger amplitude (0.8 mag $< \Delta <$ 1.0 mag) variables than smaller amplitude (0.2 mag $< \Delta <$ 0.4 mag) variables. The ratio between detection efficiencies for different amplitudes is similar for brighter sources, and the overall correction to Figure 5 is small.

We also find that the majority of sources with $\Delta >$ 0.4 mag have VR_c fainter than 16.8 mag. We note that the sources in P08 also have larger amplitudes, generally greater than 0.4 mag. A histogram of only the SuperMACHO LMC candidates with $\Delta > 0.4$ mag also indicates an excess of subluminous sources similar to that observed by P08 (Figure 7). We suggest that the subluminous population described in P08 may reflect these larger amplitude sources.

As discussed in P08, the explanation for these sources remains an open question. We note that the separation between the main and subluminous populations observed by P08 is similar to that observed in these data. Given the differences in the compositions and star-formation histo-

ries of Fornax and LMC, this similarity lends support to the conclusion that these large amplitude, subluminous sources evolved from the same population as those on the main PL-relation. It would otherwise be difficult to explain why both galaxies have such similar larger amplitude, subluminous populations that evolved independently.

CONCLUSION

We present 2323 candidate HADS in the Large Magellanic Cloud (LMC). We find evidence for a large set of FO pulsators within this data set. Notably, the PL-relation defined by the FO pulsators does not show a clear separation from the PL-relation defined by the F pulsators. This is not necessarily surprising, as δ-Scuti occupy a region of the instability strip that spans a broad region of temperatures, and hence intrinsic color. We also find that the majority of our HADS with amplitudes greater than 0.4 mag lie below the ridgeline of the PL-diagram. By examining only these candidates, we find an excess of subluminous sources similar to that observed in Fornax (P08).

ACKNOWLEDGMENTS

The SuperMACHO survey was undertaken under the auspices of the NOAO Survey Program. We are grateful for the support provided to this program from the NOAO and the National Science Foundation. We are also indebted to the scientists and staff at the Cerro Tololo Inter-American Observatory. SuperMACHO is supported by the STScI grant GO-10583. We are grateful to members of the ESSENCE supernova survey and the High Performance Technical Computing staff at Harvard. This work was performed under the auspices of the U.S. DOE by LLNL under Contract DE-AC52-07NA27344.

*References

1. C. Alcock, R. A. Allsman, D. R. Alves, T. S. Axelrod, A. C. Becker, D. P. Bennett, K. H. Cook, N. Dalal, A. J. Drake, K. C. Freeman, M. Geha, K. Griest, M. J. Lehner, S. L. Marshall, D. Minniti, C. A. Nelson, B. A. Peterson, P. Popowski, M. R. Pratt, P. J. Quinn, C. W. Stubbs, W. Sutherland, A. B. Tomaney, T. Vandehei, and D. Welch, *ApJ* **542**, 281–307 (2000).
2. E. Poretti, G. Clementini, E. V. Held, C. Greco, M. Mateo, L. Dell'Arciprete, L. Rizzi, M. Gullieuszik, and M. Maio, ApJ **685**, 947–957 (2008).
3. A. Rest, C. Stubbs, A. C. Becker, G. A. Miknaitis, A. Miceli, R. Covarrubias, S. L. Hawley, R. C. Smith, N. B. Suntzeff, K. Olsen, J. L. Prieto, R. Hiriart, D. L. Welch, K. H. Cook, S. Nikolaev, M. Huber, G. Prochtor, A. Clocchiatti, D. Minniti, A. Garg, P. Challis, S. C. Keller, and B. P. Schmidt, *ApJ* **634**, 1103–1115 (2005).
4. A. Garg, C. W. Stubbs, P. Challis, W. M. Wood-Vasey, S. Blondin, M. E. Huber, K. Cook, S. Nikolaev, A. Rest, R. C. Smith, K. Olsen, N. B. Suntzeff, C. Aguilera, J. L. Prieto, A. Becker, A. Miceli, G. Miknaitis, A. Clocchiatti, D. Minniti, L. Morelli, and D. L. Welch, *AJ* **133**, 403–419 (2007).
5. G. Miknaitis, G. Pignata, A. Rest, W. M. Wood-Vasey, S. Blondin, P. Challis, R. C. Smith, C. W. Stubbs, N. B. Suntzeff, R. J. Foley, T. Matheson, J. L. Tonry, C. Aguilera, J. W. Blackman, A. C. Becker, A. Clocchiatti, R. Covarrubias, T. M. Davis, A. V. Filippenko, A. Garg, P. M. Garnavich, M. Hicken, S. Jha, K. Krisciunas, R. P. Kirshner, B. Leibundgut, W. Li, A. Miceli, G. Narayan, J. L. Prieto, A. G. Riess, M. E. Salvo, B. P. Schmidt, J. Sollerman, J. Spyromilio, and A. Zenteno, *ApJ* **666**, 674–693 (2007).
6. A. Garg, *Microlensing candidate selection and detection efficiency for the SuperMACHO Dark Matter search*, Ph.D. thesis, Harvard University (2008).
7. A. Rest, and A. Garg, "Detecting Rare Events in the Time-Domain," in *American Institute of Physics Conference Series*, edited by C. A. L. Bailer-Jones, 2008, vol. 1082 of *American Institute of Physics Conference Series*, pp. 294–301.
8. C. Alard, and R. H. Lupton, *ApJ* **503**, 325–+ (1998).
9. C. Alard, *A&AS* **144**, 363–370 (2000).
10. J. D. Reimann, *Frequency Estimation Using Unequally-Spaced Astronomical Data*, Ph.D. thesis, University of California, Berkeley (1994).
11. G. Foster, AJ **109**, 1889–1902 (1995).
12. P. Reegen, A&A **467**, 1353–1371 (2007).
13. G. Bono, R. Incerpi, and M. Marconi, ApJ **467**, L97+ (1996).
14. R. F. Stellingwerf, A. Gautschy, and R. J. Dickens, ApJ **313**, L75–L79 (1987).
15. D. H. McNamara, PASP **112**, 1096–1102 (2000).